CHEMISTRY
AN ASIAN JOURNAL

DOI: 10.1002/asia.201200629

Enzyme Immobilization and Direct Electrochemistry Based on a New Matrix of Phospholipid-Monolayer-Functionalized Graphene

Jiyang Liu,[a] Lei Han,[a] Tianshu Wang,[a, b] Wei Hong,[a] Yaqing Liu,*[a] and Erkang Wang*[a]

Abstract: A new nanocomposite material for enzyme immobilization and subsequent direct electrochemistry and electrocatalysis was developed by using 1,2-dimyristoyl-sn-glycero-3-phospho-(1-*rac*-glycerol)-phospholipid-monolayer-membrane-modified graphene (DMPG-G). Microperoxidase-11 (MP11) was chosen as a model enzyme to investigate the composite system. Owing to the improved conductivity and biocompatible microenvironment, MP11 that was immobilized in the matrix of the DMPG-G nanocomposite (DMPG-G-MP11) effectively retained its native structure and bioactivity. DMPG-G-MP11-modified glassy carbon electrode (DMPG-G-MP11/GCE) exhibited a pair of well-defined quasi-reversible redox peaks of MP11 and showed high electrocatalytic activity towards hydrogen peroxide (H_2O_2). The linear response of the developed biosensor for the determination of H_2O_2 ranged from 2.0×10^{-6} to 4.5×10^{-4} M with a detection limit of 7.2×10^{-7} M. This biosensor exhibited high reproducibility and long-term storage stability. The promising features of this biosensor indicate that these lipid–graphene nanocomposites are ideal candidate materials for the direct electrochemistry of redox proteins and that they could serve as a versatile platform for the construction of a third-generation biosensor.

Keywords: biocatalysis · electrochemistry · graphene · monolayers · phospholipids

Introduction

Graphene, as a new polyaromatic molecule, has attracted considerable attention in recent years in materials science and biotechnology.[1–4] Because of its large specific surface area, low manufacturing cost, great mechanical strength, and high thermal and electrical conductivities, graphene has been intensively investigated for applications in nanocomposites,[5,6] nanoelectronic devices,[7] biosensors,[8–10] field-effect transistors,[11] and supercapacitors.[12] However, owing to the strong π–π-stacking interactions, pristine graphene sheets generally show poor water solubility and tend to form irreversible agglomerates,[13] and this has obviously limited its biochemical applications. Recently, a major goal in graphene chemistry has been its bio-functionalization for imparting graphene with aqueous solubility and biocompatibility, with the aim of exploiting new graphene materials in biological and medicinal applications.

Biomembranes in living organisms consist of lipids, proteins, and carbohydrates. It has been shown that mimetic biomembranes can be prepared by casting aqueous liposome onto the surface of electrodes. Because lipid films can provide an excellent biological microenvironment, they have remained a focus of study in recent years and their remarkable biocompatibility has prompted their application as one of the most promising matrixes for protein immobilization.[14–16] Potential applications based on lipid–protein composites include electrochemical biosensing platforms.[17–19] It is expected that a new material that is formed from a combination of a biocompatible lipid with graphene might have potential applications for synthesizing suitable materials that can provide a favorable microenvironment to maintain the activity of the bound proteins and for direct electrochemistry. However, to the best of our knowledge, the fabrication and direct electrochemistry of biosensors that are based on phospholipid-monolayer-modified graphene nanomaterials have only been rarely reported.

Herein, we report a new phospholipid-monolayer-membrane/graphene bionanocomposite and demonstrate its application in enzyme immobilization and subsequent direct electrochemistry. This composite was synthesized according to a facile non-covalent-modification strategy through the chemical reduction of graphene oxide in the presence of a solution of 1,2-dimyristoyl-sn-glycero-3-phospho-(1-*rac*-glycerol) (DMPG) liposomes. The assembled phospholipid-monolayer membranes, which are biologically relevant

[a] J. Liu, L. Han, T. Wang, W. Hong, Dr. Y. Liu, Prof. E. Wang
State Key Laboratory of Electroanalytical Chemistry
Changchun Institute of Applied Chemistry
Chinese Academy of Sciences
Changchun, Jilin 130022 (China)
Graduate School of the Chinese Academy of Sciences
Beijing, 100039 (China)
Fax: (+86) 431-85689711
E-mail: yaqingliu@ciac.jl.cn
ekwang@ciac.jl.cn

[b] T. Wang
College of Physics
Jilin University
Changchun 130012 (P. R. China)

supramolecular structures, impart graphene with excellent biocompatibility and aqueous solubility. Combined with the excellent electrical conductivity of graphene and the favorable biocompatibility of the phospholipids, the DMPG-monolayer-membrane-functionalized graphene (DMPG-G) may provide a favorable biological microenvironment to maintain the activity of immobilized enzymes and to realize their direct electrochemistry. Microperoxidase-11 (MP-11) was used as a model enzyme to evaluate this electrochemical platform. Owing to the favorable microenvironment and the improved conductivity, the as-prepared biosensor was successfully employed for the electrocatalytic detection of H_2O_2 and exhibited good performance.

Results and Discussion

Assembly of the phospholipid monolayer on graphene was performed through the reduction of GO by L-ascorbic acid in the presence of a solution of DMPG liposome. DMPG is a typical negatively charged phospholipid that is commonly used in the fabrication and investigation of mimetic biomembranes.[20,21] After removing any excess DMPG liposomes and L-ascorbic acid through centrifugation, we found that the individual DMPG–graphene composite could form well-dispersed aqueous colloids and showed long-term stability over several months when stored at 4 °C in a refrigerator.

UV/Vis absorption spectroscopy was used to characterize the formation of DMPG-G. As shown in Figure 1 A, two peaks for the GO dispersion are centered at 230 and 300 nm, owing to the π–π^* transition of aromatic C=C bonds and the n–π^* transition of the C=O bond, respectively.[22] After the reaction had finished, the color of the solution changes from light brown to dark, as shown in the inset of Figure 1 A. The adsorption peak at 300 nm disappears and the absorption peak of the GO dispersion at 230 nm red-shifts to 268 nm, coupled with an increase in the absorbance over the whole spectroscopic region. These results indicate that the electronic conjugation within the graphene sheets is restored upon reduction by L-ascorbic acid.[23] The modification of graphene with DMPG was also confirmed by FTIR analysis. The FTIR spectrum of DMPG-G is given in Figure 1 B, along with that of DMPG as a control reaction. We found that the FTIR spectrum of DMPG-G exhibited the typical DMPG-absorption features of the symmetric and antisymmetric CH_2 stretching vibrations at 2854 and 2920 cm^{-1}, respectively.[18,24] Thus, the attachment of DMPG molecules onto the surface of graphene was clearly confirmed.

Atomic force microscopy (AFM) was performed to further characterize the morphology of the chemically reduced graphene by L-ascorbic acid with and without DMPG. Pristine graphene showed a smooth surface and had an average thickness of 0.8 nm, which is consistent with literature data (Figure 2 A).[23] However, for DMPG-G, many segments in the membrane structure are clearly observed on the surface

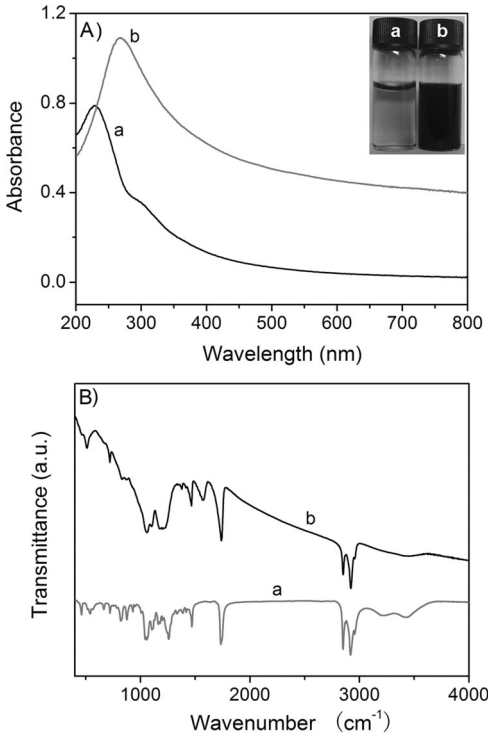

Figure 1. A) UV/Vis spectra of GO (a) and DMPG-G (b). Insets show photographs of dispersions of GO (a) and DMPG-G (b). B) FTIR spectra of DMPG (a) and DMPG-G (b).

(Figure 2 B). These segments have a very uniform height (about 2.4 nm), which corresponds to the half-height of the DMPG bilayers (4.79 nm), as reported by Tajima et al.[25] This result indicates that the DMPG molecules are oriented perpendicular to the graphene surface and form an organized monolayer. Because the surface of graphene is highly hydrophobic, it is reasonable to consider that the hydrophilic head-groups of the DMPG molecules are oriented toward the aqueous phase and that their fatty hydrophobic chains stand on the graphene through van der Waals interactions, in a similar manner to the assembly of surfactant molecules on the surface of carbon nanotubes.[26]

As MP-11 is a heme-containing protein, UV/Vis absorption spectroscopy is an effective way to examine its secondary structure because shifts in the Soret absorption band of heme may reflect its possible denaturation. Figure 3 shows the UV/Vis absorption spectra of films of dry MP11, DMPG-G, and DMPG-G-MP11 on quartz slides. An obvious absorption peak at around 410 nm (Figure 3 a) is characteristic of a dry MP11 film, thus indicating the presence of characteristic Soret absorption bands.[18] For DMPG-G (Figure 3 b), the absorption peak appears at around 268 nm, thus suggesting electronic conjugation within the graphene sheets.[4] After the immobilization of MP11 in the matrix of DMPG-G, the resultant DMPG-G-MP11 (Figure 3 c) composite film exhibits characteristic bands of both MP11 and graphene. It is worthy of note that the positions of the Soret absorption bands do not change in the obtained DMPG-G-MP11 composite film, thus implying that the immobilized

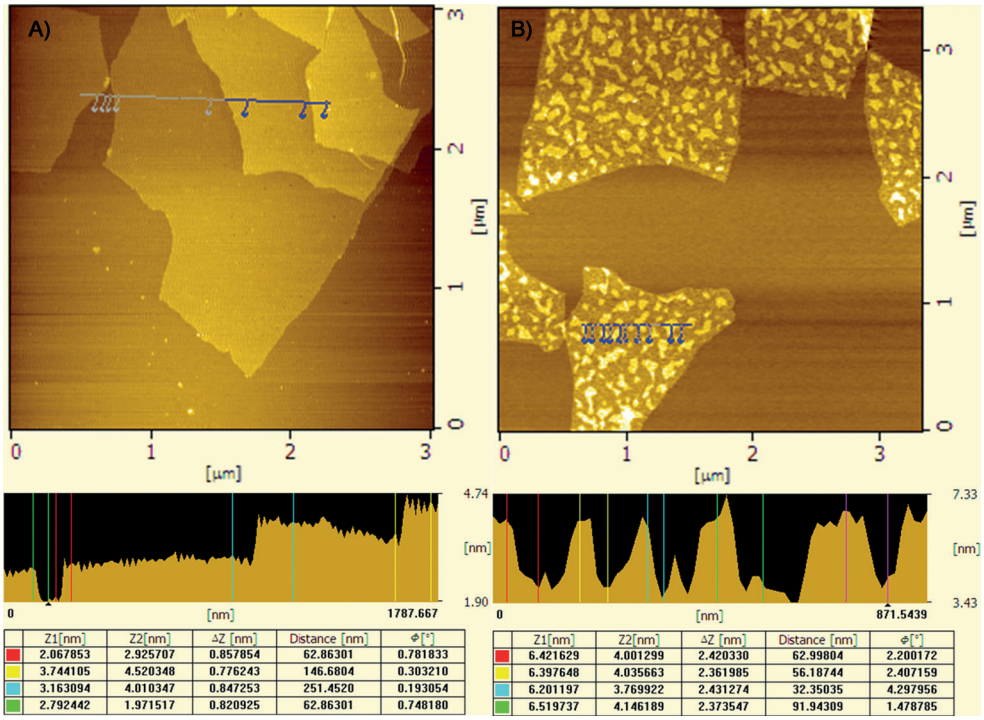

Z1[nm]	Z2[nm]	ΔZ [nm]	Distance [nm]	Φ[°]
2.067853	2.925707	0.857854	62.86301	0.781833
3.744105	4.520348	0.776243	146.6804	0.303210
3.163094	4.010347	0.847253	251.4520	0.193054
2.792442	1.971517	0.820925	62.86301	0.748180

Z1[nm]	Z2[nm]	ΔZ [nm]	Distance [nm]	Φ[°]
6.421629	4.001299	2.420330	62.99804	2.200172
6.397648	4.035663	2.361985	56.18744	2.407159
6.201197	3.769922	2.431274	32.35035	4.297956
6.519737	4.146189	2.373547	91.94309	1.478785

Figure 2. Tapping-mode AFM images of A) graphene and B) DMPG-G on freshly cleaved mica.

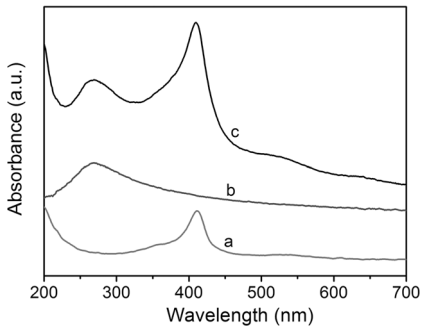

Figure 3. UV/Vis spectra of dry a) MP11 film, b) DMPG-G film, and c) DMPG-G-MP11 film on quartz slides.

MP11 retains a similar secondary structure to the MP11 film. These results indicate that the biocompatible DMPG-G material might provide a favorable microenvironment for the immobilized MP11 to maintain its activity.

MP-11 is a heme-containing undecapeptide that exhibits high electrocatalytic activity for the reduction of hydrogen peroxide.[27,28] Cyclic voltammograms (CVs) were obtained in N_2-saturated phosphate-buffered saline (PBS; 0.1 M, pH 7.0), as shown in Figure 4. No peaks were observed at the bare GCE (Figure 4 A a) and DMPG-G/GCE (Figure 4 A d), thus indicating that DMPG-G was not an electroactive material over the potential range. An increased apparent-double-layer current might result from the excellent capacitance of graphene. After MP11 was immobilized in the DMPG-phospholipid-cast film (Figure 4 A b) and in the

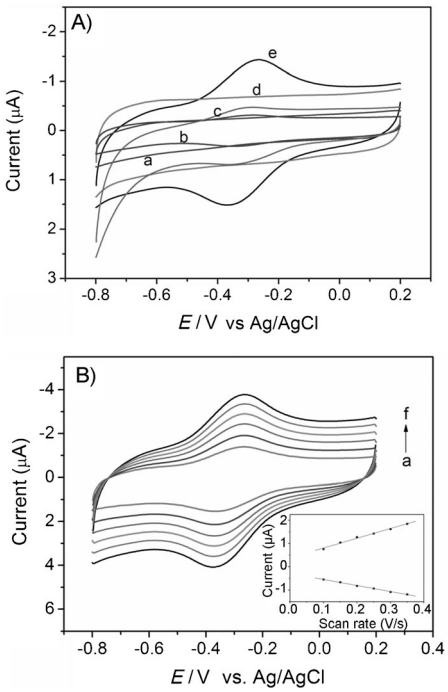

Figure 4. A) CVs of GCE (a), DMPG-MP11/GCE (b), G-MP11-GCE (c), DMPG-G/GCE (d), and DMPG-G-MP11/GCE (e) in N_2-saturated PBS (pH 7.0, 0.1 M); scan rate: 100 mV s^{-1}. B) CVs of DMPG-G-MP11/GCE in N_2-saturated PBS at scan rates of 100 (a), 150 (b), 200 (c), 250 (d), 300 (e), and 350 mV s^{-1} (f). Inset: linear dependence of the peak current on scan rate.

graphene-cast film (Figure 4 A c) on the surface of the GCE, a couple of peaks with low magnitudes were observed at −0.3 V, which corresponded to the direct electron transfer between the heme active site of MP11 and the electrode surface. When MP11 was immobilized within the matrix of graphene on the surface of the GCE, an increased current response was observed, thus indicating that the graphene matrix could facilitate electron transfer between the electroactive center of MP11 and the underlying electrode. The current response became significantly enhanced (Figure 4 A e) once MP11 was immobilized in a matrix of DMPG-G film. As estimated from the average of the anodic peak potential (−0.27 V) and the cathodic peak potential (−0.35 V), the formal potential is −0.31 V. The peak-potential separation is about 80 mV and lower than that of MP11 that is immobilized in a chitosan–graphene matrix (130 mV).[28] These results indicate a more effective electron-transfer process within the developed biosensor. These results might be ascribed to a combination of the individual benefits of the phospholipid and graphene. It is possible that the excellent electrical conductivity of graphene could facilitate the electron transfer between the electroactive center of MP11 and the underlying electrode. Moreover, the biocompatibility of the DMPG-G film forces the heme group of MP11 to adopt a favorable orientation for electron exchange with the underlying electrode. Figure 4 B shows the current response of DMPG-G-MP11/GCE as a function of scan rate. Both the reduction- and oxidation-peak currents linearly increased with increasing scan rate (Figure 4 B, inset), which revealed that the electron transfer between MP11 and the underlying electrode was a surface-controlled electrochemical process. The heterogeneous electron-transfer rate constant (k_s) of the MP11 that was immobilized in the DMPG-G matrix was estimated by using the Laviron equation.[29] The average k_s was determined to be 2.19 ($\pm$0.34) s^{-1}, which is larger than a previously reported value (1.27 s^{-1}),[30] thus indicating a more effective electron transfer between the redox-active sites of MP11 and the underlying electrode.

MP11 is commonly used as sensing template for the catalytic reduction of H_2O_2. Figure 5 A shows the electrocatalytic response of the biosensor towards H_2O_2 in N_2-saturated PBS. The concentrations of H_2O_2 were 0, 40, 80, 120, 160, 200, 240, and 280 μM, respectively. In the absence of H_2O_2, the direct electrochemistry of the immobilized MP11 demonstrated a pair of well-defined redox peaks. With the consecutive addition of H_2O_2, the cathodic peak current increased significantly; this increase contributed to the catalytic reduction of H_2O_2 by the surface-confined MP11. Accompanying the reduction of H_2O_2, the surface-confined MP11 was correspondingly oxidized. Thus, in the reverse potential scan, the anodic peak current that originated from the oxidation of MP11 gradually decreased and finally disappeared on increasing the concentration of H_2O_2. Figure 5 B shows a plot of the cathodic peak current as a function of H_2O_2 concentration; a wide linear range from 2.0×10^{-6} to 4.5×10^{-4} M with a correlation coefficient of 0.9997 was obtained

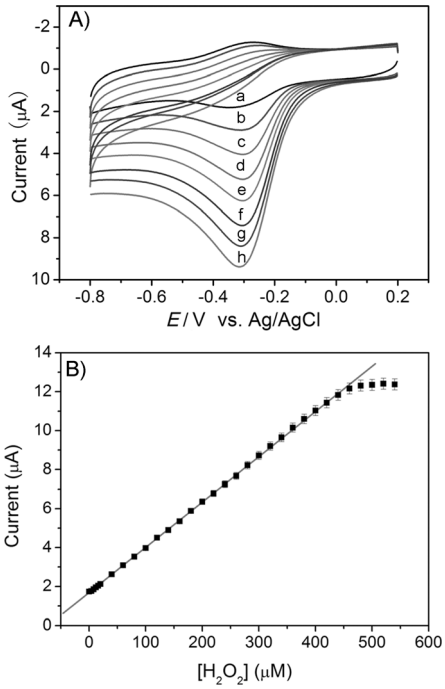

Figure 5. A) Bioelectrocatalysis of DMPG-G-MP11/GCE towards H_2O_2 in PBS at a scan rate of 0.1 $V s^{-1}$ and H_2O_2 concentrations of 0 (a), 40 (b), 80 (c), 120 (d), 160 (e), 200 (f), 240 (g), and 280 μM (h). B) Linear relationship between catalytic current and the concentration of H_2O_2. The error bars represent the relative standard deviation (RSD) of three measurements.

and the detection limit of the electrode was estimated to be 7.2×10^{-7} M based on a signal/noise ratio of 3. The apparent Michaelis–Menton constant (K_m) was estimated according to the Lineweaver–Burk equation.[30] The K_m value and the maximum electrode sensitivity (I_{max}/K_m) were evaluated to be 0.34 mM and 50.6 μA mM^{-1}, respectively. The K_m value was similar to that of MP11/GNPs/MWNTs/GCE (0.32 mM)[30] and lower than those of MP11/MGN-CHI/Au (0.54 mM)[28] and MP11-HCPE (6.4 mM).[32] This result indicates that the DMPG-G-MP11/GC electrode possesses high catalytic efficiency for the reduction of H_2O_2. Compared with H_2O_2 sensors that were based on HRP immobilized in a DMPG-lipid-bilayer membrane,[33] hemoglobin immobilized in egg-phosphatidylcholine-lipid-cast film,[17] and MP11 immobilized in chitosan/graphene composite,[28] the remarkable wider detection range and lower detection limit of DMPG-G-MP11/GC confirm that this as-prepared phospholipid-membrane/graphene bionanomaterial can provide a favorable microenvironment for an immobilized enzyme to present excellent catalytic properties.

The reproducibility of the biosensor was evaluated by recording the response towards 80 μM H_2O_2 over five successive CV measurements. The relative standard deviation (RSD) of the results was 2.1%. Six biosensors were independently prepared under the same conditions to evaluate electrode-to-electrode reproducibility. A RSD of 5.3% was obtained, which indicated a good reproducibility of the developed biosensor. The stability of the fabricated biosensor

was investigated by comparison of the initial peak current with that obtained after time intervals of 24 h. The decrease in the intensity of the peak was 1.0%, thus indicating good stability. The catalytic current response maintained about 91% of its original response over a 20 day period when the modified electrode was stored at 4°C in a refrigerator under dry conditions. The good reproducibility and stability can be ascribed to the unique biocompatibility of the DMPG-G composite material.

Conclusions

DMPG-G, with its good aqueous solubility and biocompatibility, provides a new host matrix for enzyme immobilization and for the construction of electrochemical biosensors. Owing to the good biocompatibility of DMPG and the excellent electrical conductivity of graphene, MP11 that is entrapped in the DMPG-G matrix presents high electrocatalytic activity, as well as good stability and reproducibility, for the detection of H_2O_2. A wide detection range, from 2.0×10^{-6} to 4.5×10^{-4} M, and a detection limit as low as 7.2×10^{-7} M have been obtained. The high sensitivity, good stability, and electrocatalytic activity towards substrates suggest that the DMPG-G is promising for potential applications in third-generation biosensors. By combining the unique properties of graphene and the phospholipid-monolayer membrane, the DMPG-G bio-composite is expected to find potential applications in biomimetics and in drug-delivery systems.

Experimental Section

Chemicals

1,2-Dimyristoyl-sn-glycero-3-phosphatidil glycerol (DMPG) was purchased from Avanti Polar Lipids, Inc. (Alabaster, AL). Microperoxidase-11, from horse heart cytochrome c and L-ascorbic acid, were purchased from Sigma (USA). Graphite was purchased from Alfa Aesar. H_2O_2 was obtained from Beijing Chemical Reagent Factory (Beijing, China). A fresh solution of H_2O_2 was prepared daily. Unless otherwise stated, other reagents were of analytical grade and used as received. All aqueous solutions were prepared by using ultrapure water (18.2 MΩ cm^{-1}) from a Milli-Q Plus system (Millipore).

Apparatus and Measurements

AFM was performed by using a SPI3800N microscope (Seiko Instruments, Inc.). UV/Vis absorption spectroscopy measurements were carried out on a Cary 50 UV/Vis spectrophotometer (Varian, USA). Zeta potentials (effective surface charge) were measured by dynamic light scattering (Zeta-sizer 3000, Malvern Instruments, France). FTIR was performed on a Bruker Vertex 70 FTIR spectrometer. Electrochemical experiments were carried out at room temperature on a CHI 602a electrochemical workstation (Shanghai Chenhua Equipment, China) in phosphate-buffered saline solution (PBS; 0.1 M, pH 7.0). A standard three-electrode system was employed for the electrochemical measurements with a platinum-wire auxiliary electrode, a Ag/AgCl (saturated KCl) reference electrode, and a modified glassy carbon electrode (GCE) as the working electrode. The buffer solutions were purged with purified nitrogen for 20 min to remove oxygen prior to the start of the experiments.

Preparation of DMPG Liposomes

The unilamellar DMPG liposomes were prepared according to modified procedures reported by Fujimoto et al.[34] Briefly, DMPG (8 mg) was dissolved in $CHCl_3$/MeOH (1:1 v/v, 1 mL). Then, $CHCl_3$ and MeOH were evaporated and dried under vacuum overnight. The resulting dry lipid film was rehydrated with doubly distilled water (16 mL). The resulting liposome suspension was sonicated in a 25°C bath sonicator until a clear suspension of liposomes was formed. The finally obtained negatively charged liposome was denoted as DMPG liposome.

Preparation of Phospholipid-Monolayer-Membrane-Functionalized Graphene

Graphite oxide was prepared from natural graphite according to Hummers method with little modification.[35] DMPG-G was prepared as follows: A dispersion of GO in water (1 mg mL^{-1}, 2 mL) was added to a solution of DMPG liposome in water (0.5 mg mL^{-1}, 16 mL), and the mixture was sonicated for 20 min in a 25°C sonicator bath to form a uniformly light-yellow dispersion. A solution of L-ascorbic acid in water (10 mg mL^{-1}, 2 mL) was added to the mixed solution under vigorous stirring and the obtained solution was kept at 40°C in a water bath for 24 h. Finally, the resulting stable black dispersion was centrifuged (14000 rpm) and washed three times with water to remove the excess DMPG liposomes and L-ascorbic acid. The obtained nanocomposites, denoted as DMPG-G, were then re-suspended in water and stored at 4°C in a refrigerator.

Preparation of the DMPG-G-MP11-Modified Electrode

A glassy carbon electrode (diameter: 3.0 mm) was polished with 1.0 μm, 0.3 μm, and 0.05 μm α-alumina slurries, sonicated in doubly distilled water for 1 min, and dried under a flow of nitrogen. Solutions of DMPG-G (0.2 mg mL^{-1}, 0.5 mL) and MP-11 (0.2 mg mL^{-1}, 0.5 mL) in water were mixed together, and a portion of the mixture (5 μL) was transferred by syringe onto the freshly polished GCE and dried at 4°C in a refrigerator. The obtained electrode was denoted as DMPG-G-MP11/GCE. DMPG-G/GCE, G-MP11/GCE, and DMPG-MP11/GCE were prepared according to similar procedures and used in control experiments.

Acknowledgements

This work was supported by the National Natural Science Foundation of China (Grant Nos. 21190040 and 21105095) and by the 973 Project (Nos. 2010CB933600 and 2009CB930100).

[1] X. Li, X. Wang, L. Zhang, S. Lee, H. Dai, *Science* **2008**, *319*, 1229.
[2] S. Stankovich, D. A. Dikin, G. H. B. Dommett, K. M. Kohlhaas, E. J. Zimney, E. A. Stach, R. Piner, S. Nguyen, R. Ruo, *Nature* **2006**, *442*, 282.
[3] W. Ren, Y. Fang, E. Wang, *ACS Nano* **2011**, *5*, 6425.
[4] D. Li, M. Muller, S. Gilje, R. Kaner, G. Wallace, *Nat. Nanotechnol.* **2008**, *3*, 101.
[5] A. Patil, J. Vickery, T. Scott, S. Mann, *Adv. Mater.* **2009**, *21*, 3159.
[6] Y. Guo, S. Guo, J. Ren, Y. Zhai, S. Dong, E. Wang, *ACS Nano* **2010**, *4*, 4001.
[7] Y. Sui, J. Appenzeller, *Nano Lett.* **2009**, *9*, 2973.
[8] Y. Guo, L. Deng, J. Li, S. Guo, E. Wang, S. Dong, *ACS Nano* **2011**, *5*, 1282.
[9] Y. Song, Y. Chen, L. Feng, J. Ren, X. Qu, *Chem. Commun.* **2011**, *47*, 4436.
[10] C. Shan, H. Yang, D. Han, Q. Zhang, A. Ivaskab, L. Niu, *Biosens. Bioelectron.* **2010**, *25*, 1070.
[11] S. Gilje, S. Han, M. Wang, K. Wang, R. Kaner, *Nano Lett.* **2007**, *7*, 3394.
[12] Y. Wang, Z. Shi, Y. Huang, Y. Ma, C. Wang, M. Chen, Y. Chen, *J. Phys. Chem. C* **2009**, *113*, 13103.
[13] Y. Xu, H. Bai, G. Lu, C. Li, G. Shi, *J. Am. Chem. Soc.* **2008**, *130*, 5856.

[14] Z. Shenkarev, E. Lyukmanova, A. Paramonov, L. Shingarova, V. Chupin, M. Kirpichnikov, M. Blommers, A. Arseniev, *J. Am. Chem. Soc.* **2010**, *132*, 5628.
[15] C. Gutiérrez-Sánchez, D. Olea, M. Marques, V. Fernández, I. Pereira, M. Vélez, A. De Lacey, *Langmuir* **2011**, *27*, 6449.
[16] D. Dutta, A. Pulsipher, M. Yousaf, *Langmuir* **2010**, *26*, 9835.
[17] X. Han, W. Huang, J. Jia, S. Dong, E. Wang, *Biosens. Bioelectron.* **2002**, *17*, 741.
[18] G. Li, X. Liu, L. Du, E. Wang, *Electroanalysis* **2008**, *20*, 1421.
[19] J. Tang, B. Wang, Z. Wu, X. Han, S. Dong, E. Wang, *Biosens. Bioelectron.* **2003**, *18*, 867.
[20] K. Hall, T. Leeand, M. Aguilar, *J. Mol. Recognit.* **2011**, *24*, 108.
[21] M. Nieh, V. Raghunathan, G. Pabst, T. Harroun, K. Nagashima, H. Morales, J. Katsaras, P. Macdonald, *Langmuir* **2011**, *27*, 4838.
[22] P. Ang, S. Wang, Q. Bao, J. Thong, K. Loh, *ACS Nano* **2009**, *3*, 3587.
[23] J. Zhang, H. Yang, G. Shen, P. Cheng, J. Zhang, S. Guo, *Chem. Commun.* **2010**, *46*, 1112.
[24] X. Liu, L. Zhang, Y. Wang, C. Guo, E. Wang, *Cryst. Growth Des.* **2008**, *8*, 759.
[25] K. Tajima, Y. Imai, A. Nakamura, M. Koshinuma, *Adv. Colloid Interface Sci.* **2000**, *88*, 79.
[26] C. Richard, F. Balavoine, P. Schultz, T. Ebbesen, C. Mioskowski, *Science* **2003**, *300*, 775.
[27] Z. Chen, D. Sun, Y. Zhou, J. Zhao, T. Lu, X. Huang, C. Cai, J. Shen, *Biosens. Bioelectron.* **2011**, *29*, 53.
[28] Y. Zhou, S. Liu, H. Jiang, H. Yang, H. Chen, *Electroanalysis* **2010**, *22*, 1323.
[29] E. Laviron, *J. Electroanal. Chem.* **1974**, *52*, 355.
[30] Y. Liu, M. Wang, F. Zhao, Z. Guo, H. Chen, S. Dong, *J. Electroanal. Chem.* **2005**, *581*, 1.
[31] R. Kamin, G. Wilson, *Anal. Chem.* **1980**, *52*, 1198.
[32] V. Razumas, J. Kazlauskaite, R. Vidziunaite, *Bioelectrochem. Bioenerg.* **1996**, *39*, 139.
[33] Z. Wu, B. Wang, Z. Cheng, X. Yang, S. Dong, E. Wang, *Biosens. Bioelectron.* **2001**, *16*, 47.
[34] K. Fujimoto, T. Toyoda, Y. Fukui, *Macromolecules* **2007**, *40*, 5122.
[35] Y. Li, Y. Wu, *J. Am. Chem. Soc.* **2009**, *131*, 5851.

Received: July 18, 2012
Revised: August 20, 2012
Published online: October 2, 2012

